

# **Environment-Sensitive Azepane-Substituted $\beta$ -Diketones and Difluoroboron Complexes with Restricted C-C Bond Rotation**

*Fang Wang, Christopher A. DeRosa, Daniel Song, Diane A. Dickie, Cassandra L. Fraser\**

Department of Chemistry, University of Virginia, Charlottesville, Virginia 22904, USA

\*Corresponding author: [fraser@virginia.edu](mailto:fraser@virginia.edu)

## ABSTRACT

Luminescent  $\beta$ -diketones (bdks) and difluoroboron coordinated complexes ( $\text{BF}_2\text{bdks}$ ) exhibit many environment-sensitive properties, such as solvatochromism, viscochromism, aggregation-induced emission (AIE), thermal and mechanochromic luminescence (ML). In a previous study, an azepane-substituted bdk ligand (L1) and boron dye (D1) showed noteworthy luminescence properties but low quantum yields ( $\Phi$ , L1: 0.26; D1: 0.02) due to free intramolecular bond rotation and twisted intramolecular charge transfer (TICT) state formation with associated non-radiative decay. Thus, in order to improve the quantum yields, an azepane-substituted bdk ligand (L2) and boron complex (D2) with restricted C-C bond rotation were synthesized and various luminescence properties were investigated. Restricting bond rotation blue-shifted absorptions and emissions, increased lifetimes and greatly improved quantum yields ( $\Phi$ , L2: 0.47; D2: 0.83). Excited state density functional theory (DFT) calculations displayed twisted geometries for L1 and D1 but more planar geometries for L2 and D2. All compounds showed red-shifted emissions in more polar solvents. For viscochromism, L1 and D1 exhibited higher emission intensity in more viscous media. However, L2 and D2 did not show dramatic viscochromism, substantiating the relation between viscosity sensitivity and intramolecular bond twisting. Additionally, while both ligands showed quenched emission upon aggregation, the dyes exhibited AIE regardless of bond restriction. Thermal and ML studies showed a more dramatic emission shift for L2 than L1 between thermally annealed (TA) and melt quenched (MQ) states. In summary, the quantum yields of the azepane substituted bdk ligand and boron dye were successfully improved by restricting intramolecular C-C bond rotation, making various luminescent properties more promising for environment-sensitive applications.

## INTRODUCTION

Small organic molecules with luminescence have been widely studied and utilized in biological imaging and sensing applications.<sup>1</sup> Environment-sensitive dyes show responsive luminescence signals when local properties change, and have attracted increasing attention in recent years.<sup>2</sup> Among these, solvatochromic dyes display different emission colors in response to solvent polarity changes.<sup>2</sup> Upon excitation, intramolecular charge transfer (ICT) from an electron donor group to an acceptor produces a dipolar excited state, which can interact with different solvent dipoles and result in varying emission wavelengths.<sup>3</sup> Therefore, dyes with solvatochromism have been used in sensing and probing model membrane polarity as well as in living cells.<sup>4,5</sup> Dyes with another type of environment-sensitive property, viscochromism, show different emission intensities responding to local viscosity change.<sup>2</sup> Such dyes possess a freely rotating bond in the structure, and after light excitation, a twisted intramolecular charge transfer (TICT) state is formed with bond rotation, leading to enhanced non-radiative decay.<sup>6,7</sup> In more viscous environments, enhanced emission intensity is observed due to restricted bond rotation. Thus, viscochromic dyes can be used to probe lipid and cell membranes.<sup>8,9</sup> For example, Kuimova *et al.* utilized a boron dipyrromethene (BODIPY) dye and fluorescence lifetime imaging microscopy (FLIM) to sense and image cell membrane viscosities.<sup>10</sup>

In addition to dye sensitivity to solvent polarity and viscosity, dye emission can also be affected by solubility. In poor solvents, aggregation of organic dyes can lead to quenched emission, known as aggregation caused quenching (ACQ), enhanced emission, namely aggregation induced emission (AIE), or unaffected emission.<sup>11</sup> While the ACQ effect is caused by  $\pi$ - $\pi$  interactions of molecules, dyes with AIE properties show enhanced emission due to restriction of intramolecular motions (RIM), comprised of restriction of intramolecular rotations (RIR) and restriction of

intramolecular vibrations (RIV).<sup>12,13</sup> Utilizing the turn-on fluorescence property, applications of AIE dyes include biosensing lipids, carbohydrates, amino acids, proteins, enzymes and nucleic acids.<sup>14</sup> In the solid state, mechanochromic luminescent (ML) dyes show sensitivity to internal environment change (*i.e.*, different packing modes) after smearing, grinding, heating or melt quenching.<sup>15,16</sup> Previous studies show that while smearing, grinding or melt quenching leads to more amorphous packing of dyes, heating or thermally annealing typically results in more crystalline states.<sup>17,18</sup> Dyes with ML properties exhibit differing emission colors between crystalline and amorphous states,<sup>19</sup> and show applications as mechanical sensors and light-emitting diodes.<sup>15</sup>

Difluoroboron  $\beta$ -diketone ( $\text{BF}_2\text{bdk}$ ) dyes show promising optical properties including multiphoton absorption, color tunable emission and high quantum yield.<sup>20</sup> Recently, an azepane substituted  $\beta$ -diketone (bdk) (L1) and difluoroboron complex (D1) were synthesized and studied, showing noteworthy environment-sensitive and multi-stimuli responsive luminescent properties and great promise in biological applications.<sup>21</sup> However, the quantum yields of the azepane ligand and boron dye are relatively low (*i.e.*, 0.26 for L1 and 0.02 for D1), which is not ideal for sensing and imaging use, since quantum yield and brightness are critical for fluorescent probing and imaging.<sup>1,22</sup> Therefore, in order to improve the quantum yields of the azepane ligand and boron dye, a new azepane substituted  $\beta$ -diketone ligand (L2) and difluoroboron coordinated complex (D2) were synthesized by adding a methylene bridge in the structure and restricting the C-C bond rotation between the azepane substituted phenyl ring and the central diketone moiety (Figure 1). Since intramolecular bond rotation leads to formation of TICT states and non-radiative decay when excited,<sup>6</sup> it is probable that restriction of the C-C bond rotation in this study could effectively decrease non-radiative relaxation and greatly improve the quantum yield. The optical properties

of the bdk ligand and boron dye were measured in  $\text{CH}_2\text{Cl}_2$  and compared to those of unrestricted azepane compounds. Solvatochromism, viscochromism, AIE, thermal and ML experiments were also conducted for comparison.

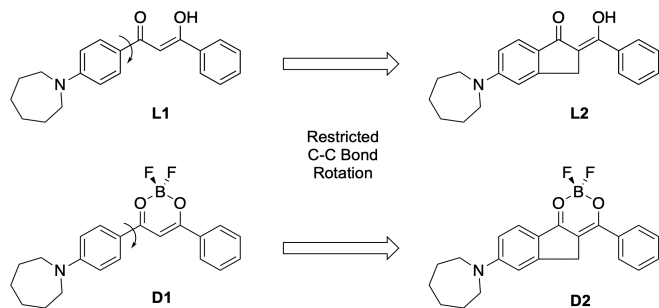


**Figure 1.** Chemical structures of azepane substituted  $\beta$ -diketones and difluoroboron complexes before and after restricting C-C bond rotation.

## EXPERIMENTAL SECTION

### Materials

Solvents used in synthesis,  $\text{CH}_2\text{Cl}_2$  and THF, were dried over activated 3  $\text{\AA}$  molecular sieves using a previously described method.<sup>23</sup> Reagent grade chemicals in this study were purchased from TCI, Alfa Aesar and Sigma-Aldrich, and used without further purification. Reactions were monitored by silica TLC plates. Before synthesis of the  $\beta$ -diketone ligand, the azepane substituted ketone was prepared as the starting material using a previously reported method.<sup>24</sup>

### Methods

$^1\text{H}$  NMR spectra were collected on a Varian NMRS 600 (600 MHz) instrument in  $\text{CDCl}_3$ . Peaks were referenced to the residual protiochloroform signal at 7.26 ppm, and coupling constant units were in Hz. Mass spectrometry was conducted using a Micromass Q-TOF Ultima

spectrometer with electrospray ionization method (ESI). Steady-state fluorescence spectra were measured on a Horiba Fluorolog-3 Model FL3-22 spectrofluorometer with double-grating excitation and a double-grating emission monochromator. UV-Vis spectra were recorded with a Hewlett-Packard 8452A diode-array spectrophotometer. Fluorescence quantum yield of the restricted azepane bdk ligand L2 was measured in  $\text{CH}_2\text{Cl}_2$  against a dilute solution of quinine sulfate in 0.1 M  $\text{H}_2\text{SO}_4$  as a standard using a previously described method,<sup>25</sup> with the values:  $\lambda_{\text{ex}} = 366$  nm,  $\phi_F$  (quinine sulfate in 0.1 M  $\text{H}_2\text{SO}_4$ ) = 0.53,<sup>25,26</sup>  $n_{\text{D}}^{20}$  (0.1 M  $\text{H}_2\text{SO}_4$ ) = 1.333,  $n_{\text{D}}^{20}$  ( $\text{CH}_2\text{Cl}_2$ ) = 1.424.<sup>27</sup> A different standard, rhodamine 6G in EtOH, was used for quantum yield measurement of the restricted boron dye D2 in  $\text{CH}_2\text{Cl}_2$ ,<sup>25</sup> with the following values:  $\lambda_{\text{ex}} = 488$  nm,  $\phi_F$  (rhodamine 6G in EtOH) = 0.94,<sup>28</sup>  $n_{\text{D}}^{20}$  (EtOH) = 1.361,  $n_{\text{D}}^{20}$  ( $\text{CH}_2\text{Cl}_2$ ) = 1.424.<sup>27</sup> Time-correlated single photon counting (TCSPC) fluorescence lifetimes were measured using a DataStation HUB as the SPC controller, and a NanoLED-370 as the excitation source ( $\lambda_{\text{ex}} = 369$  nm). Lifetime data analysis was performed using DataStation v2.4 software from Horiba Jobin Yvon. Differential scanning calorimetry (DSC) for the pristine powder of L2 was conducted utilizing a TA Instruments DSC 2920 Modulated DSC. Thermograms were recorded with a 5 °C/min temperature ramp rate using the standard mode. A second cycle was completed for reporting after the first conditioning scan. Data for DSC was analyzed using the Universal Analysis Software V 2.3 from TA Instruments.

## Computational Details

The Gaussian 09 suite of programs was utilized for DFT calculations of all the azepane bdk ligands and boron complexes.<sup>29</sup> For ground state calculations, optimized molecular geometries were obtained using B3LYP/6-31+G(d) and a Tomasi polarized continuum model in

dichloromethane.<sup>30</sup> Vibrational frequencies were calculated utilizing B3LYP/6-31+G(d) as well, and the ground state geometry was treated as a local minimum only when all the frequency numbers were positive. Single point energy calculations using B3LYP/6-31G(d) were then conducted to obtain the molecular orbital diagrams, and GaussView 5 software was utilized to visualize the orbitals.<sup>31</sup> Time-dependent density functional theory (TD-DFT) calculations with TD-B3LYP/6-311+G(d) were performed to predict absorption spectra of all the azepane bdk ligands and boron dyes. For all the excited state calculations, TD-B3LYP/6-31+G(d) was used to achieve optimized geometries and vibrational frequencies.

### **Environment-Sensitive Property Measurements**

Stock solutions in  $\text{CH}_2\text{Cl}_2$  were prepared for the restricted azepane bdk ligand L2 and boron complex D2 during solvatochromism, viscochromism and AIE studies. Appropriate volumes of the stock solutions were then transferred to empty vials, after which the solvent  $\text{CH}_2\text{Cl}_2$  was allowed to evaporate in air. Solvents with different polarities for solvatochromism experiments, DMSO/acetonitrile or dioxane/EtOAc with different ratios for viscochromism, and different compositions of water/THF for AIE studies were then added into the vials to obtain a series of solutions with a concentration of  $10^{-5}$  M. UV-excited images, and absorption and emission spectra of the solutions were then recorded. In the solid state, thermal and ML properties of the azepane ligand L2 were studied. After smearing  $\sim$ 10-20 mg powder on weighing paper, the sample-covered paper was then thermally annealed (TA) in an oven at  $110\text{ }^\circ\text{C}$  for 10 min. After taking a picture under UV light and recording an emission spectrum in the TA state, a heat gun was used to melt the sample for  $\sim$ 10 s, and the weighing paper was allowed to cool in air for 5 min. A UV-excited image and emission spectrum in the melt quenched (MQ) state were then obtained.

## Synthesis Details

Protons on the azepane substituted phenyl ring are labeled as primed.

*(Z)-5-(azepan-1-yl)-2-(hydroxy(phenyl)methylene)-2,3-dihydro-1H-inden-1-one* (L2). The azepane substituted ketone, 5-(azepan-1-yl)-2,3-dihydro-1H-inden-1-one (306 mg, 1.3 mmol), and methyl benzoate (167  $\mu$ L, 1.3 mmol), were dissolved in anhydrous THF (20 mL). A suspension of sodium hydride in oil dispersion (60%, 160 mg, 4.0 mmol) in anhydrous THF (10 mL) was added to the reaction mixture by cannula transfer. The reaction was refluxed at 70 °C under N<sub>2</sub> for 18 h. After the ketone was completely consumed, which was confirmed by TLC, the mixture was allowed to cool to room temperature, and then was quenched by adding 1 M HCl (5 mL). The THF solvent was removed by rotary evaporation. The crude product was then extracted with EtOAc (2  $\times$  20 mL), followed by water (2  $\times$  20 mL) and brine (2  $\times$  20 mL) washes. For each extraction and wash, 1 M HCl (5 mL) was added to keep the mixture acidic. The organic fraction was then dried with anhydrous Na<sub>2</sub>SO<sub>4</sub>. After filtration, the solvent was removed by rotary evaporation. The crude product was purified by recrystallization (CH<sub>2</sub>Cl<sub>2</sub>/hexanes) and silica gel chromatography (hexanes/EtOAc 5:1) to yield a yellow solid: 140.9 mg, 31.7 %. <sup>1</sup>H NMR (600 MHz, CDCl<sub>3</sub>):  $\delta$  14.85 (s, 1H, -OH), 7.89 (d,  $J$  = 6, 2H, 2, 6-ArH), 7.71 (d,  $J$  = 12, 1H, 6'-ArH), 7.58 (t,  $J$  = 6, 1H, 4-ArH), 7.50 (t,  $J$  = 6, 2H, 3, 5-ArH), 6.75 (d,  $J$  = 6, 1H, 5'-ArH), 6.70 (s, 1H, 3'-ArH), 3.83 (s, 2H, Ar-CH<sub>2</sub>CCO-), 3.55 (t,  $J$  = 6, 4H, Ar-N(CH<sub>2</sub>CH<sub>2</sub>CH<sub>2</sub>-)<sub>2</sub>), 1.82 (s, 4H, Ar-N(CH<sub>2</sub>CH<sub>2</sub>CH<sub>2</sub>-)<sub>2</sub>), 1.58-1.55 (m, 4H, Ar-N(CH<sub>2</sub>CH<sub>2</sub>CH<sub>2</sub>-)<sub>2</sub>). HRMS (ESI, TOF) *m/z* calculated for C<sub>22</sub>H<sub>24</sub>NO<sub>2</sub>, 334.1807 [M + H]<sup>+</sup>; found 334.1813.

*(Z)-5-(azepan-1-yl)-2-(((difluoroboraneyl)oxy)(phenyl)methylene)-2,3-dihydro-1H-inden-1-one* (D2). The restricted boron dye was synthesized by dissolving the corresponding bdk ligand L2 (93 mg, 0.28 mmol) in anhydrous CH<sub>2</sub>Cl<sub>2</sub> (20 mL), and boron trifluoride diethyl etherate (45  $\mu$ L, 0.36

mmol) was added using syringe. The mixture was stirred at room temperature under N<sub>2</sub> for 16 h. After complete consumption of the reagent, as monitored by TLC, cold methanol (-20 °C, 80 mL) was added to precipitate the solid product. After stirring for 15 min, the mixture was filtered and the crude product was purified by recrystallization (CH<sub>2</sub>Cl<sub>2</sub>/hexanes) to yield a red solid: 82.7 mg, 77.8 %. <sup>1</sup>H NMR (600 MHz, CDCl<sub>3</sub>):  $\delta$  8.05 (d, *J* = 6, 2H, 2, 6-ArH), 7.80 (d, *J* = 12, 1H, 6'-ArH), 7.53 (t, *J* = 6, 1H, 4-ArH), 7.49 (t, *J* = 6, 2H, 3, 5-ArH), 6.81 (d, *J* = 6, 1H, 5'-ArH), 6.74 (s, 1H, 3'-ArH), 3.94 (s, 2H, Ar-CH<sub>2</sub>CCO-), 3.61 (t, *J* = 6, 4H, Ar-N(CH<sub>2</sub>CH<sub>2</sub>CH<sub>2</sub>-)<sub>2</sub>), 1.59-1.57 (m, 4H, Ar-N(CH<sub>2</sub>CH<sub>2</sub>CH<sub>2</sub>-)<sub>2</sub>), 1.54 (s, 4H, Ar-N(CH<sub>2</sub>CH<sub>2</sub>CH<sub>2</sub>-)<sub>2</sub>). HRMS (ESI, TOF) *m/z* calculated for C<sub>22</sub>H<sub>21</sub>BF<sub>2</sub>NO<sub>2</sub>, 380.1633 [M - H]<sup>-</sup>; found 380.1634.

## RESULTS AND DISCUSSION

### Synthesis and Optical Properties

The azepane substituted bdk ligand (L2) was prepared by Claisen condensation as previously reported,<sup>32</sup> and the corresponding boron complex (D2) was synthesized *via* boronation utilizing boron trifluoride diethyl etherate.<sup>33</sup> Optical properties of the compounds including UV-Vis absorption maxima ( $\lambda_{\text{abs}}$ ), fluorescence maxima ( $\lambda_{\text{em}}$ ), quantum yield ( $\phi$ ), extinction coefficient ( $\epsilon$ ) and fluorescence lifetime ( $\tau$ ) were measured for 10<sup>-5</sup> M CH<sub>2</sub>Cl<sub>2</sub> solutions (see Table 1). Comparing the bdk ligand L2 to the corresponding D2 boron dye, D2 displayed more red-shifted absorption and emission, a higher quantum yield and extinction coefficient, and a longer fluorescence lifetime than L2. This trend is consistent with a previous study.<sup>34</sup> Versus the unrestricted parent compounds L1 and D1, the absorptions of both L2 and D2 blue-shifted, and though the ligand extinction coefficients were similar, D2 displayed a lower extinction coefficient than D1 by ~7 000 M<sup>-1</sup>cm<sup>-1</sup>. While the emission of L2 slightly red-shifted versus L1, the fluorescence of D2 blue-shifted compared to D1. The azepane compounds with restricted bond

rotation displayed much longer fluorescence lifetimes and dramatically higher quantum yields (*i.e.*,  $\Phi$ : L1, 0.26; L2, 0.47; D1, 0.02; D2, 0.83), demonstrating the effectiveness of improving dye quantum yield by restricting intramolecular bond rotation.

**Table 1.** Optical properties of the azepane substituted bdk ligands and boron dyes in  $\text{CH}_2\text{Cl}_2$

Compound	$\lambda_{\text{abs}}^a$ (nm)	$\varepsilon^b$ ( $\text{M}^{-1}\text{cm}^{-1}$ )	$\lambda_{\text{em}}^c$ (nm)	$\Phi^d$	$\tau^e$ (ns)
L1 <sup>f</sup>	412	37 800	491	0.26	1.16
L2	403	38 300	496	0.47	2.57
D1 <sup>f</sup>	471	61 500	543	0.02	1.20
D2	467	54 700	528	0.83	3.73

<sup>a</sup> Absorbance maxima in air.  
<sup>b</sup> Extinction coefficient.  
<sup>c</sup> Fluorescence maxima in air ( $\lambda_{\text{ex}} = 369$  nm).  
<sup>d</sup> Quantum yield.  
<sup>e</sup> Fluorescence lifetime in air ( $\lambda_{\text{ex}} = 369$  nm).  
<sup>f</sup> Data taken from Ref. 21.

## Computational Studies

For all the bdk ligands and boron dyes, lifetime analysis showed double exponential decay (Figure S4), and multiple peaks were found in the absorption spectra (Figure S2a). These indicate multiple energy transitions were present during the light excitation process. Density functional theory (DFT) calculations were conducted to explore optimized geometries, energy transitions and frontier molecular orbitals (FMOs) (Figures 2 and 3, Tables S1 and S2). The main energy transitions are determined to be the highest occupied molecular orbital (HOMO) to the lowest unoccupied molecular orbital (LUMO) and HOMO-1 to LUMO according to the oscillator strength (f) data in Table S1. The HOMO to LUMO transition is the dominant energy transition because of greater oscillator strength (*e.g.*, L2, f is 0.8433 for HOMO to LUMO and 0.2777 for HOMO-1 to LUMO) (Table S1). As shown in Figure 2, for all the compounds, ground state DFT

calculation results show electron density is mainly centered on the azepane substituted phenyl ring in the HOMO. For orbital HOMO-1, electron density is localized on the central diketone moiety as well as the unsubstituted phenyl ring, and electron density is delocalized on the whole molecule in the LUMO. The primary energy transition (HOMO to LUMO) supports the presence of ICT in all the compounds. Multiple transitions, such as HOMO to LUMO and HOMO-1 to LUMO, in turn account for the double exponential decay in lifetime measurements and the different peaks in the absorption spectra.

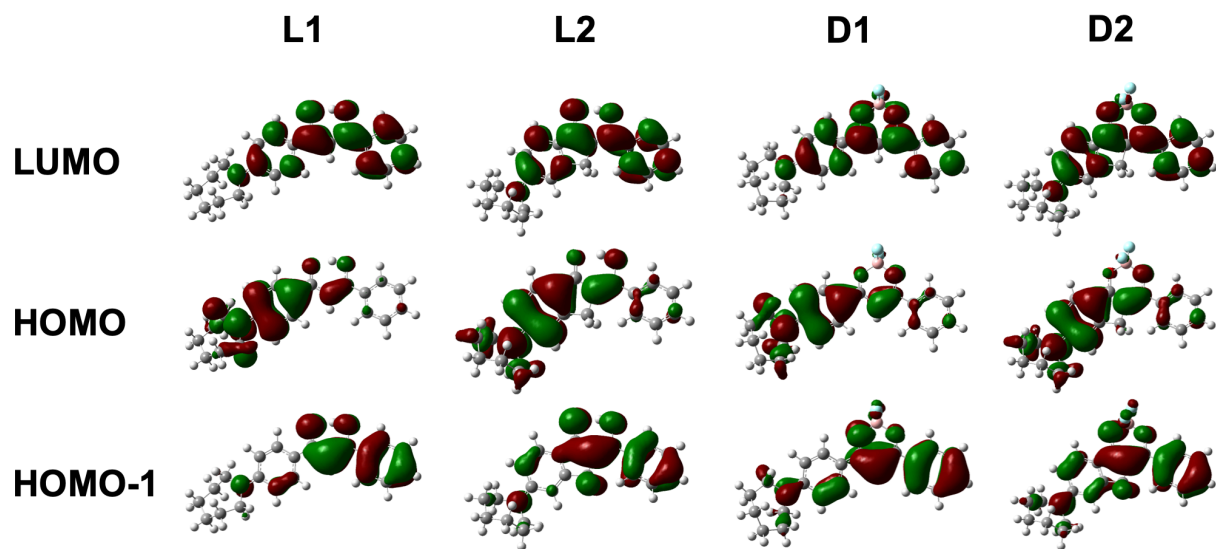


**Figure 2.** Ground state DFT calculations: molecular orbitals of all the bdk ligands and boron dyes. Data for L1 and D1 was taken from Ref. 21.

Time-dependent density functional theory (TD-DFT) calculations were conducted for the excited state to investigate the optimized geometry change after restriction of C-C bond rotation. As Figure 3 shows, upon light excitation, the unrestricted azepane ligand (L1) and boron dye (D1) adopt a twisted optimized geometry in the excited state, while L2 and D2 with restriction of bond rotation show more planar geometries across the entire conjugation length. This further supports

the formation of TICT states upon light excitation for the bdk ligand and boron complex with intramolecular bond rotation.

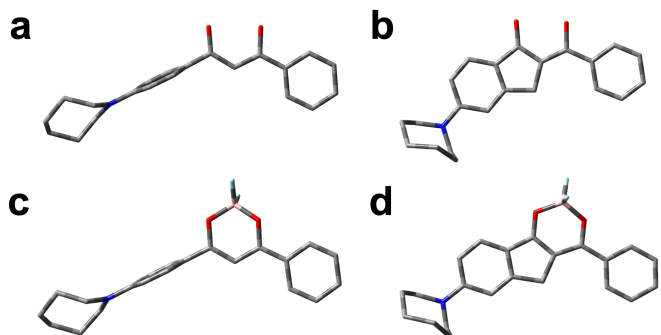


**Figure 3.** Optimized excited state geometries of (a) L1, (b) L2, (c) D1 and (d) D2. Hydrogens are omitted for clarity. Image (c) was taken from Ref. 21.

### Solvatochromism

Intramolecular charge transfer in the restricted azepane ligand and boron dye often correlates with solvatochromism properties.<sup>2,3</sup> Thus, solvatochromism experiments were conducted in a series of solvents with different polarities,  $E_T(30)$  value ranging from 33.7 for toluene to 46 for acetonitrile.<sup>35,36</sup> Absorption and emission spectra, and images under UV light excitation were taken with the same concentration of  $10^{-5}$  M for all solvents. In a previous study, the unrestricted azepane ligand and boron complex showed red-shifted emission in more polar solvents but exhibited dark emission in polar solvents (*e.g.*, acetone, methanol and acetonitrile), due to the formation of TICT states and more non-radiative decay from the excited state.<sup>21</sup> According to Figure S5, for all the compounds, similar absorption wavelengths were shown in the differing solvents, suggesting ground state energies are unaffected by solvent polarity changes. As is shown in Figure 4, UV-excited images and emission spectra were obtained under the same experimental settings for L1 and L2. Compared to L1, restriction of C-C bond rotation in L2 dramatically increased the emission intensities in various solvents, and brighter emissions were

observed in acetone, methanol and acetonitrile, where L1 showed dark emissions. In more polar solvents, both bdk ligands exhibited bathochromic emissions, which is positive solvatochromism. The highest emission intensity was observed in dioxane for both azepane ligands regardless of bond restriction. In toluene, L1 and L2 showed the most blue-shifted emissions. While L1 displayed the most red-shifted emission in methanol, the reddest emission for L2 was in acetonitrile.

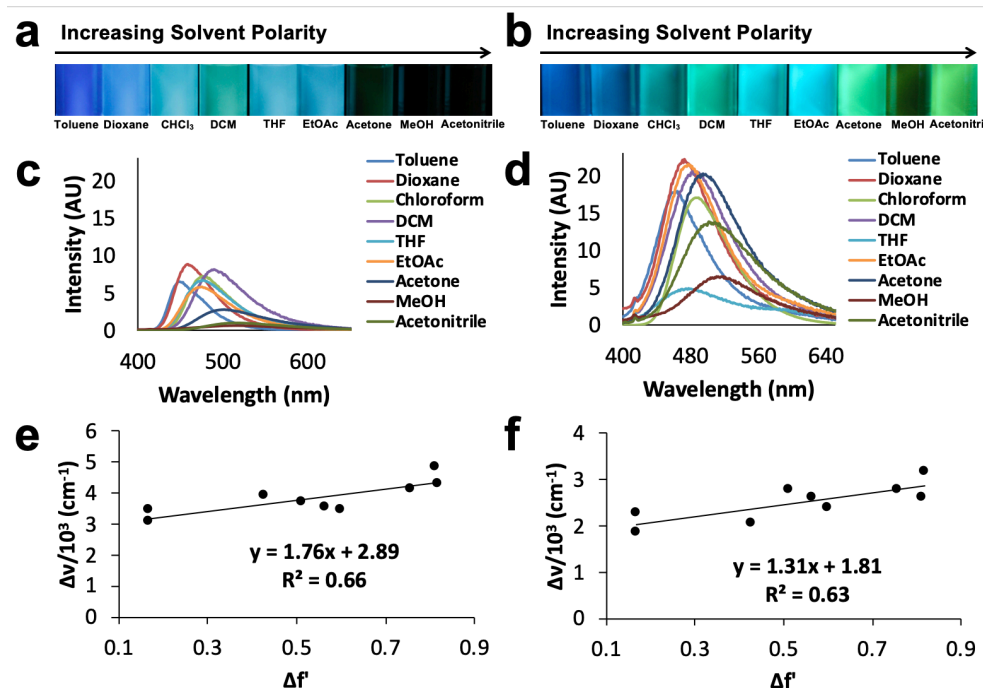


**Figure 4.** Solvatochromism: UV-excited images of (a) L1 and (b) L2 in different solvents, and emission spectra of (c) L1 and (d) L2. The same camera settings were used when taking the images of L1 and L2 under UV light. The same excitation ( $\lambda_{ex} = 369$  nm) and slit wavelength (1.5 nm) were used in emission measurements. Lippert-Mataga plots of (e) L2 and (f) D2. Data for L1 was taken from Ref. 21.

Because the TICT state was present, Lippert-Mataga plots of Stokes shifts ( $\Delta\nu$ ) versus solvent orientational polarizability ( $\Delta f'$ ) were used,<sup>37</sup> and  $\Delta f'$  was calculated using the following equation:

$$\Delta f' = \frac{\varepsilon - 1}{\varepsilon + 2} - \frac{n^2 - 1}{2n^2 + 4}$$

where  $\epsilon$  is the relative dielectric constant and  $n$  is the solvent refractive index. A linear relationship with a positive slope was shown in the Lippert-Mataga plots (Figure 4e,f), further demonstrating positive solvatochromism for the azepane substituted bdk ligand and boron dye with restricted C-C bond rotation.

### Viscochromism

In viscochromism experiments of the azepane substituted boron complexes, the solvents dioxane and EtOAc, were selected for their similar polarities ( $E_T(30)$  values: 36 kcal mol<sup>-1</sup> and 38.1 kcal mol<sup>-1</sup> respectively), but different viscosities (1.37 cP for dioxane and 0.45 cP for EtOAc at 20 °C).<sup>36</sup> This approach minimizes solvatochromism effects during viscochromism studies, as verified by Lippert-Mataga plots (Figure S8). According to Figure 5, the fluorescence intensity of D1 decreased with increasing EtOAc (*i.e.*, lower viscosity), due to a more freely rotating intramolecular bond and TICT state formation. After restriction of C-C bond rotation, D2 did not show a dramatic emission intensity change in different solvent viscosities compared to the unrestricted boron dye. Similar experiments were conducted with the azepane ligands, but a different solvent pair was used, namely, DMSO and acetonitrile, with similar polarities ( $E_T(30)$  values: 45 kcal mol<sup>-1</sup> for DMSO and 46 kcal mol<sup>-1</sup> for acetonitrile),<sup>36</sup> and differing viscosities (1.996 cP for DMSO and 0.3417 cP for acetonitrile at 25 °C).<sup>38</sup> For the unrestricted ligand L1, increased fluorescence intensity was observed in solvent mixtures with higher DMSO fractions. However, the emission intensity of L2 was unresponsive to solvent viscosity change (Figure S7). These results indicate the relation between sensitivity to viscosity change and intramolecular bond rotation, and in turn, substantiate the hypothesis that restriction of bond rotation can effectively decrease TICT state formation and non-radiative decay, and consequently improve quantum yield.

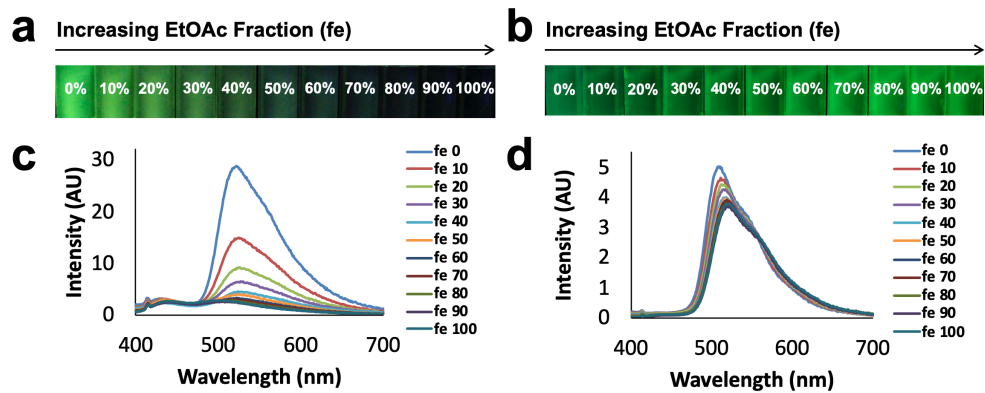


**Figure 5.** Viscochromism: UV-excited images of (a) D1 and (b) D2 in solvent mixtures with different fractions of EtOAc (fe), and emission spectra of (c) D1 and (d) D2 ( $\lambda_{\text{ex}} = 369$  nm). Data for D1 was taken from Ref. 21.

### Aggregation Induced Emission

In addition to environment-sensitive properties in solution, sensitivity of the azepane ligands and boron dyes to aggregation was also investigated. Miscible water and THF were selected as the solvent pair used in the AIE experiments with the azepane ligands and dyes well soluble in THF but showing poor solubility in water, which could induce AIE. A series of water/THF compositions were prepared with percentage of water from 0% to 95%, and images under UV light, absorption and emission spectra were obtained for all the compounds dissolved in the solvent mixtures with a dye concentration of  $10^{-5}$  M (Figures 6 and S9). All the compounds aggregated at high water fractions (*i.e.*, 80%, 90% and 95%), which was supported by the dramatic signal intensity increase in the absorption spectra when water percentage was above 80% and stronger light scattering was present (Figure S10). As shown in Figure 6, for the unrestricted boron dye D1, dark states were observed at 0-70% water fractions due to intramolecular bond rotation and TICT states, with associated non-radiative decay. The emission was dramatically enhanced as well as red-shifted when the water percentage rose to above 80%, especially at 90% and 95%. For comparison, D2 with restricted C-C bond rotation still showed green emission when the water

fraction was under 70%. Emission intensity kept decreasing with adding water. Red-shifted and enhanced emission was observed when the water percentage rose above 80%. Therefore, both azepane substituted boron dyes exhibited red-shifted AIE regardless of the C-C bond rotation restriction, but the difference was, while D1 showed dark emissions, bright green emissions were observed for D2 at water fractions under 70%. For the azepane bdk ligands, similar experiments were conducted. According to Figure S9, both ligands showed slightly blue-shifted emission and diminished fluorescence intensity when aggregated.

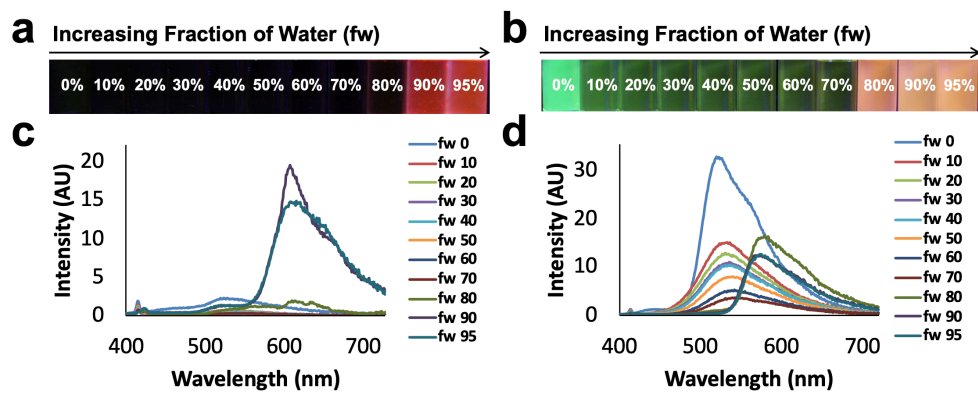


**Figure 6.** UV-excited images of (a) D1 and (b) D2 in water/THF mixtures with different fractions of water (fw), and emission spectra of (c) D1 and (d) D2 ( $\lambda_{\text{ex}} = 369$  nm). Data for D1 was taken from Ref. 21.

### Thermal and Mechanochromic Properties

In the solid state, thermal and ML properties were investigated on weighing paper to explore the sensitivity of the azepane ligand to molecular packing. Because the boron dyes D1 and D2 were not mechano-active upon preliminary screening, the bdk ligands L1 and L2 serve as the focus of this investigation. Thermally annealed (TA) and melt quenched (MQ) samples were prepared on weighing paper, and UV excited images and emission spectra were collected. Typically, thermally annealing causes samples to form more crystalline states,<sup>17</sup> and melt quenching results in amorphous states with red-shifting emission.<sup>39,40</sup> Differential scanning

calorimetry (DSC) curves of the azepane ligands were obtained (Figure S11), and the crystallization temperature ( $T_c$ ) and melting point ( $T_m$ ) were determined. The thermal annealing temperature (110 °C) was set in between the crystallization and melting points.<sup>33</sup> According to Figure 7, the unrestricted azepane ligand L1 did not show an emission wavelength shift but only peak broadening after melt quenching the thermally annealed sample weighing paper. However, compared to L2 in the TA state, dramatic red-shifted emission (45 nm) was observed for the restricted ligand after melt quenching. To reveal packing details of molecules, single crystals of L2 was grown by vapor diffusion of *n*-pentane into a THF solution, for comparison with the crystal structure of L1 in the previous study.<sup>21</sup> As is shown in Figure 8, while multiple pairs of offset dimers are found in the unit cell of L2, the unrestricted ligand L1 packs in a herringbone pattern with no dimers present. This is consistent with previous studies showing mechanochromic luminescence for bdk compounds that form face-to-face or offset dimers.<sup>16</sup>

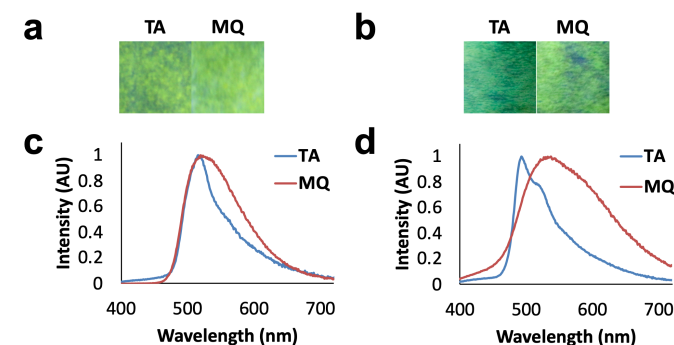


**Figure 7.** UV-excited images of (a) L1 and (b) L2, and emission spectra of (c) L1 and (d) L2 weighing papers in thermally annealed (TA) and melt quenched (MQ) states ( $\lambda_{\text{ex}} = 369$  nm). Data for L1 was taken from Ref. 21.

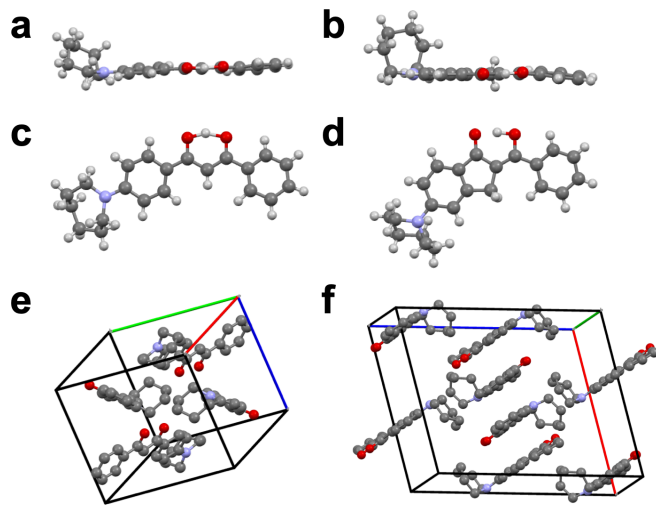


**Figure 8.** Single crystal structures of (a) L1 and (b) L2 from the top view, and (c) L1 and (d) L2 from the side view. Unit cells of (e) L1 and (f) L2. Hydrogens are deleted for clarity. Data for L1 was taken from Ref. 21.

## CONCLUSION

In summary, an azepane-substituted  $\beta$ -diketone ligand and the corresponding boron complex with restricted intramolecular C-C bond rotation were synthesized to improve the quantum yields compared to the unrestricted analogues. This molecular design strategy was successful. In  $\text{CH}_2\text{Cl}_2$ , blue-shifted absorption and emission maxima as well as dramatically increased quantum yields and lifetimes were observed after restricting the bond rotation. Ground state DFT calculations showed intramolecular charge transfer from HOMO to LUMO for all the azepane ligands and dyes. In the excited state, computational studies showed completely twisted geometries for the unrestricted ligand and dye, and the bdk ligand and boron complex with restricted bond rotation adopted more planar geometries. Various environment-sensitive properties were investigated for the restricted bdk ligand and boron dye, and compared to those of unrestricted compounds. All the compounds were solvatochromic and displayed red-shifted emission in more polar solvents regardless of bond restriction. Viscochromism studies, however, showed higher

emission intensity for the unrestricted ligand and dye in more viscous media, compared to restricted compounds that showed little to no response to solvent viscosity change. This underscores the relationship between intramolecular bond rotation and viscosity sensitivity. For AIE experiments, the boron dyes exhibited enhanced emission in the aggregate state, whereas, the ligands showed quenched emission when aggregated. In the solid state, thermal and ML properties on weighing paper showed a dramatic emission wavelength shift for the restricted ligand between thermally annealed and melt quenched states, while the unrestricted ligand showed no emission wavelength shift, only peak broadening. Given the high quantum yield and brightness of environment-sensitive luminescent properties, the azepane substituted  $\beta$ -diketone ligand and boron complex with restricted C-C bond rotation show great promise for sensing and imaging.

## ASSOCIATED CONTENT

Supporting Information

Synthesis route; computational details; excitation, absorption and emission spectra in  $\text{CH}_2\text{Cl}_2$ ; lifetime profiles and fits; DSC curves; images under UV light, Lippert-Mataga plots, absorption and emission spectra in various organic solvents, dioxane/EtOAc, DMSO/acetonitrile and water/THF mixtures.

## AUTHOR INFORMATION

Corresponding Author

Email: [fraser@virginia.edu](mailto:fraser@virginia.edu)

Notes

The authors declare no competing financial interest.

## ACKNOWLEDGEMENTS

We thank the National Science Foundation (CHE 1709322) and UVA Double Hoo research grant program for support for this study.

## REFERENCES

- (1) Lavis, L. D.; Raines, R. T. Bright Ideas for Chemical Biology. *ACS Chem. Biol.* **2008**, *3*, 142–155.
- (2) Klymchenko, A. S. Solvatochromic and Fluorogenic Dyes as Environment-Sensitive Probes: Design and Biological Applications. *Acc. Chem. Res.* **2017**, *50*, 366–375.
- (3) Marini, A.; Munoz-Losa, A.; Biancardi, A.; Mennucci, B. What Is Solvatochromism? *J. Phys. Chem. B* **2010**, *114*, 17128–17135.
- (4) Demchenko, A. P.; Mély, Y.; Duportail, G.; Klymchenko, A. S. Monitoring Biophysical Properties of Lipid Membranes by Environment-Sensitive Fluorescent Probes. *Biophys. J.* **2009**, *96*, 3461–3470.
- (5) Klymchenko, A. S.; Kreder, R. Fluorescent Probes for Lipid Rafts: From Model Membranes to Living Cells. *Chem. Biol.* **2014**, *21*, 97–113.
- (6) Grabowski, Z. R.; Rotkiewicz, K.; Rettig, W. Structural Changes Accompanying Intramolecular Electron Transfer: Focus on Twisted Intramolecular Charge-Transfer States and Structures. *Chem. Rev.* **2003**, *103*, 3899–4032.
- (7) Haidekker, M. A.; Theodorakis, E. A. Molecular Rotors--Fluorescent Biosensors for Viscosity and Flow. *Org. Biomol. Chem.* **2007**, *5*, 1669–1678.
- (8) Wang, F.; Song, D.; Dickie, D. A.; Fraser, C. L. Ring Size Effects on Multi-Stimuli Responsive Luminescent Properties of Cyclic Amine Substituted  $\beta$ -Diketones and

Difluoroboron Complexes. *Chem. - An Asian J.* **2019**, *14*, 1849–1859.

(9) Kuimova, M. K. Mapping Viscosity in Cells Using Molecular Rotors. *Phys. Chem. Chem. Phys.* **2012**, *14*, 12671–12686.

(10) Kuimova, M. K.; Yahiroglu, G.; Levitt, J. A.; Suhling, K. Molecular Rotor Measures Viscosity of Live Cells via Fluorescence Lifetime Imaging. *J. Am. Chem. Soc.* **2008**, *130*, 6672–6673.

(11) Hong, Y.; Lam, J. W. Y.; Tang, B. Z. Aggregation-Induced Emission. *Chem. Soc. Rev.* **2011**, *40*, 5361–5388.

(12) Wang, H.; Zhao, E.; Lam, J. W. Y.; Tang, B. Z. AIE Luminogens: Emission Brightened by Aggregation. *Mater. Today* **2015**, *18*, 365–377.

(13) Mei, J.; Leung, N. L. C.; Kwok, R. T. K.; Lam, J. W. Y.; Tang, B. Z. Aggregation-Induced Emission: Together We Shine, United We Soar! *Chem. Rev.* **2015**, *115*, 11718–11940.

(14) Kwok, R. T. K.; Leung, C. W. T.; Lam, J. W. Y.; Tang, B. Z. Biosensing by Luminogens with Aggregation-Induced Emission Characteristics. *Chem. Soc. Rev.* **2015**, *44*, 4228–4238.

(15) Sagara, Y.; Kato, T. Mechanically Induced Luminescence Changes in Molecular Assemblies. *Nat. Chem.* **2009**, *1*, 605–610.

(16) Sun, X.; Zhang, X.; Li, X.; Liu, S.; Zhang, G. A Mechanistic Investigation of Mechanochromic Luminescent Organoboron Materials. *J. Mater. Chem.* **2012**, *22*, 17332–17339.

(17) Zhang, G.; Singer, J. P.; Kooi, S. E.; Evans, R. E.; Thomas, E. L.; Fraser, C. L. Reversible Solid-State Mechanochromic Fluorescence from a Boron Lipid Dye. *J. Mater. Chem.*

2011, 21, 8295–8299.

(18) Butler, T.; Wang, F.; Sabat, M.; Fraser, C. L. Controlling Solid-State Optical Properties of Stimuli Responsive Dimethylamino-Substituted Dibenzoylmethane Materials. *Mater. Chem. Front.* 2017, 1, 1804–1817.

(19) Ito, H.; Saito, T.; Oshima, N.; Kitamura, N.; Ishizaka, S.; Hinatsu, Y.; Wakshima, M.; Kato, M.; Tsuge, K.; Sawamura, M. Reversible Mechanochromic Luminescence of [(C<sub>6</sub>F<sub>5</sub>Au)<sub>2</sub>(μ-1,4-Diisocyanobenzene)]. *J. Am. Chem. Soc.* 2008, 130, 10044–10045.

(20) Tanaka, K.; Chujo, Y. Recent Progress of Optical Functional Nanomaterials Based on Organoboron Complexes with β-Diketonate, Ketoiminate and Diiminate. *NPG Asia Mater.* 2015, 7, 223–315.

(21) Wang, F.; Derosa, C. A.; Daly, M. L.; Song, D.; Sabat, M.; Fraser, C. L. Multi-Stimuli Responsive Luminescent Azepane-Substituted β-Diketones and Difluoroboron Complexes. *Mater. Chem. Front.* 2017, 1, 1866–1874.

(22) Antaris, A. L.; Chen, H.; Diao, S.; Ma, Z.; Zhang, Z.; Zhu, S.; Wang, J.; Lozano, A. X.; Fan, Q.; Chew, L.; et al. A High Quantum Yield Molecule-Protein Complex Fluorophore for near-Infrared II Imaging. *Nat. Commun.* 2017, 8, 1–11.

(23) Williams, D. B. G.; Lawton, M. Drying of Organic Solvents: Quantitative Evaluation of the Efficiency of Several Desiccants. *J. Org. Chem.* 2010, 75, 8351–8354.

(24) Watson, A. J. A.; Fairbanks, A. J. Ruthenium-Catalyzed Transfer Hydrogenation of Amino- and Amido-Substituted Acetophenones. *European J. Org. Chem.* 2013, 6784–6788.

(25) Heller, C. A.; Henry, R. A.; McLaughlin, B. A.; Bliss, D. E. Fluorescence Spectra and Quantum Yields. Quinine, Uranine, 9,10-Diphenylanthracene, and 9,10-

Bis(Phenylethynyl)Anthracenes. *J. Chem. Eng. Data* **1974**, *19*, 214–219.

(26) Melhuish, W. H. Quantum Efficiencies of Fluorescence of Organic Substances: Effect of Solvent and Concentration of the Fluorescent Solute. *J. Phys. Chem.* **1961**, *65*, 229–235.

(27) Saunders, J. E.; Sanders, C.; Chen, H.; Loock, H.-P. Refractive Indices of Common Solvents and Solutions at 1550 Nm. *Appl. Opt.* **2016**, *55*, 947–953.

(28) Kubin, R. F.; Fletcher, A. N. Fluorescence Quantum Yields of Some Rhodamine Dyes. *J. Lumin.* **1982**, *27*, 455–462.

(29) Gaussian 09, C.01. Frisch, M. J.; Trucks, G. W.; Schlegel, H. B.; Scuseria, G. E.; Robb, M. A.; Cheeseman, J. R.; Scalmani, G.; Barone, V.; Mennucci, B.; Petersson, G. A. et al. Gaussian, Inc., Wallingford CT, USA, **2009**.

(30) Tomasi, J.; Mennucci, B.; Cammi, R. Quantum Mechanical Continuum Solvation Models. *Chem. Rev.* **2005**, *105*, 2999–3094.

(31) GaussView, Version 5. Dennington, R.; Keith, T.; Millam, J. Semichem, Inc., Shawnee Mission KS, USA, **2009**.

(32) Liu, T.; Chien, A. D.; Lu, J.; Zhang, G.; Fraser, C. L. Arene Effects on Difluoroboron  $\beta$ -Diketonate Mechanochromic Luminescence. *J. Mater. Chem.* **2011**, *21*, 8401–8408.

(33) Morris, W. A.; Liu, T.; Fraser, C. L. Mechanochromic Luminescence of Halide-Substituted Difluoroboron  $\beta$ -Diketonate Dyes. *J. Mater. Chem. C* **2015**, *3*, 352–363.

(34) Butler, T.; Morris, W. A.; Samonina-Kosicka, J.; Fraser, C. L. Mechanochromic Luminescence and Aggregation Induced Emission of Dinaphthoylmethane  $\beta$ -Diketones and Their Boronated Counterparts. *ACS Appl. Mater. Interfaces* **2016**, *8*, 1242–1251.

(35) Pople, J. A.; Gordon, M. Molecular Orbital Theory of the Electronic Structure of Organic Compounds. I. Substituent Effects and Dipole Moments. *J. Am. Chem. Soc.* **1967**, *89*,

4253–4261.

(36) Werner, T. C.; Lyon, D. B. Empirical Measures of Solvent Effects on the Fluorescence Energy of Methyl Anthroates. *J. Phys. Chem.* **1982**, *86*, 933–939.

(37) Cao, C.; Liu, X.; Qiao, Q.; Zhao, M.; Yin, W.; Mao, D.; Zhang, H.; Xu, Z. A Twisted-Intramolecular-Charge-Transfer (TICT) Based Ratiometric Fluorescent Thermometer with a Mega-Stokes Shift and a Positive Temperature Coefficient. *Chem. Commun.* **2014**, *50*, 15811–15814.

(38) Grande, C.; García, M.; Marschoff, C. M. Density and Viscosity of Anhydrous Mixtures of Dimethylsulfoxide with Acetonitrile in the Range (298.15 to 318.15) K. *J. Chem. Eng. Data* **2009**, *54*, 652–658.

(39) Zhang, G.; Lu, J.; Sabat, M.; Fraser, C. L. Polymorphism and Reversible Mechanochromic Luminescence for Solid-State Difluoroboron Avobenzone. *J. Am. Chem. Soc.* **2010**, *132*, 2160–2162.

(40) Zhang, G.; Lu, J.; Fraser, C. L. Mechanochromic Luminescence Quenching: Force-Enhanced Singlet-to-Triplet Intersystem Crossing for Iodide-Substituted Difluoroboron-Dibenzoylmethane- Dodecane in the Solid State. *Inorg. Chem.* **2010**, *49*, 10747–10749.

## TOC Graphic

